A CONSIDERATION OF LOW-SPEED DYNAMIC STALL ONSET

by

M.W. GRACEY
A.J. NIVEN
R.A.McD. GALBRAITH

Dept. of Aerospace Engineering
University of Glasgow
Glasgow, G12 8QQ, UK

FIFTEENTH EUROPEAN ROTORCRAFT FORUM

SEPTEMBER 12 - 15, 1989   AMSTERDAM

A CONSIDERATION OF LOW-SPEED DYNAMIC STALL ONSET

M. W. Gracey
A. J. Niven
R.A. McD. Galbraith

UNIVERSITY OF GLASGOW

ABSTRACT

The paper discusses relevant and contemporary criteria for the onset of low-speed dynamic stall. A new correlation is proposed which attempts to relate an aerofoil's dynamic stall onset incidence to particular parameters which describe its static stall behaviour. The correlation is derived from two parameters which are obtained under steady conditions from experimental data: the static-stall incidence, and an additional variable related to the trailing-edge separation characteristics. To generate the coefficients in the resulting equation, a large amount of aerodynamic data was analysed from experiments performed under static, ramp, and sinusoidal motions in the University of Glasgow's "Handley-Page" wind tunnel, and stored in a database. A number of aerofoils from two families have been tested: the NACA four-digit series of symmetrical sections, and a new family of four profiles, developed at the University, which has the NACA 23012 as the generic shape. The paper also discusses the outcome of a comparison between an indicial-response dynamic stall model and the experimental data specific to one of the modified NACA 23012 sections.

A, B, C, D :	constant coefficients in correlation equation
C_m :	coefficient of pitching moment about quarter chord
C_n :	coefficient of force normal to chord
C_n' :	ersatz coefficient of force normal to chord
C_{n1} :	critical coefficient of force normal to chord
C_p :	pressure coefficient
C_{pcrit} :	critical pressure coefficient at 0.25% chord
C_t :	coefficient of force tangential to chord, defined positive in direction towards leading edge
c :	length of aerofoil chord, in metres
c_1, c_2, c_3 :	constant coefficients in equations defining offset of linear stall onset relation
$F_1(.)$:	function in equation defining gradient of linear stall onset relation
f :	value of x/c at separation point
f_{max}, f_{min} :	constant coefficients in separation equations
i, j :	constant coefficients in correlation equation
K_1, K_2 :	constant coefficients in separation equations
M_∞ :	Mach number
m_1, m_2 :	constant coefficients in equations defining gradient of linear stall onset relation
p :	Laplace transform variable
R :	Re x 10^{-6}
Re :	Reynolds number
r :	reduced pitch rate, $r = (\dot{\alpha}c/2U_\infty) \, (\pi/180)$
S_1, S_2 :	constant coefficients in separation equations
T_p :	pressure compensation time constant
U_{pcrit} :	critical peak velocity at leading edge
U_∞ :	freestream velocity
x :	chordwise distance from leading edge, in metres
α :	angle of attack, in degrees

$\dot{\alpha}$:	pitch rate, in degrees per second
α_1 :	constant coefficient in separation equations
α_c :	critical angle for break in pitching moment, in degrees
α_{ds} :	angle of earliest observation that stall onset has occurred, in degrees
α_{ss} :	static stall incidence, in degrees
ΔC_m :	divergence from unstalled C_m when calculating α_c
Δt :	time delay, in seconds
τ :	non-dimensional time delay, $\tau = U_\infty \Delta t/c$
τ_{vb} :	vortex development time delay

1. INTRODUCTION

The phenomenon of aerofoil dynamic stall has challenged aerodynamicists for many years. Numerous experiments (e.g., Carr et al [1], McCroskey et al [2]) have established that two predominant features of dynamic stall are the overshoot of lift with respect to the static stall value and the shedding of a strong vortex from the upper-surface leading-edge region. The contemporary understanding of this process is illustrated in Figure 1. The dominating nature of the shed vortex over the unsteady airloads has established the determination of its initiation mechanism as a fundamental aspect of dynamic stall research. The work of McCroskey et al [3] represents one of the first experimental investigations, via hot-wire anemometers, into the nature of the boundary layer prior to vortex shedding. Four boundary-layer phenomena were identified as possible vortex inception mechanisms (dynamic stall triggers): the bursting of the laminar separation bubble; the appearance of transonic flow at the leading edge ($M_\infty > 0.2$); the abrupt breakdown of the turbulent flow over the forward portion of the aerofoil; the arrival, at the leading-edge region, of a thin stratum of reversed flow travelling upstream from the trailing edge. As suggested by McCroskey et al [2], the first two mechanisms may be categorised as leading edge, whilst the latter pair as abrupt trailing edge and trailing edge respectively. This terminology will also be adopted in the present paper. A detailed review of these vortex inception mechanisms is given by Young [4].

Part of the aerodynamic research at the University of Glasgow concentrates on the experimental investigation of dynamic stall. This is essentially achieved via extensive wind-tunnel testing from which the resulting data are stored in a database. The main portion of the database relates to unsteady aerodynamic data covering ten aerofoils for a variety of motion types, e.g. "static", "ramp", and oscillatory. Seven aerofoils, which are illustrated in Figure 2, have been tested in the manner described in Section 2. The symmetric sections were primarily of interest to the field of wind turbine aerodynamics and the others are the NACA 23012 with three derivatives. The NACA 23012A and NACA 23012C are 12% thick and, over the first 25% chord are identical to the NACA 23012 but with modifications thereafter [5,6]. The NACA 23012B is a 16% thick composite aerofoil, derived from the NACA 23012 and an RAE section [7].

The aims of the present paper are to discuss experimental techniques used to investigate vortex initiation, and to address the problem of predicting the incidence at which this occurs. A new correlation is proposed which attempts to relate an aerofoil's dynamic stall onset incidence to particular parameters which describe its static stall behaviour. The motivation for the correlation came from two sources. Firstly, there was a desire to utilise available theoretical techniques for predicting an aerofoil's steady characteristics. Secondly, there is a desire to develop easily calculable procedures for predicting vortex initiation during dynamic stall. When included in semi-empirical dynamic stall models, this correlation may be used to assist in the preliminary design stages of an aerofoil geometry which is required to display a particular characteristic under unsteady conditions. At present, detailed comparisons have been made between an indicial-response dynamic stall model and the experimental data specific to one of the modified NACA 23012 sections. The paper will discuss the outcome of this comparison which has indicated that, if the leading-edge velocity distribution is assumed to

trigger the initial boundary-layer breakdown, there exists a finite time within which this region of disturbed flow develops into a vortex structure causing a distortion of the local chordwise pressure distribution.

2. EXPERIMENTAL APPARATUS AND PROCEDURE

The test facility has been described by Leishman [8]. A diagram of the data acquisition and control system which is described in this section is sketched in Figure 3.

The models, of chord length 0.55m and span 1.61m, were constructed of a fibre-glass skin filled with epoxy resin foam bound to an aluminium spar. Each model was mounted vertically in the University of Glasgow's "Handley Page" wind tunnel which is a low speed (max speed = 57m/sec) closed - return type with a 1.61 x 2.13m octagonal working section (see Figure 4). The model was pivoted about the quarter chord using a linear hydraulic actuator and crank mechanism. The input signal to the actuator controller was provided by a function generator, comprising a BBC microcomputer and two 12-bit digital to analogue convertors: one to control the shape of the motion, and the other to set the desired voltage governing the amplitude or arc length of the motion.

Thirty ultra-miniature pressure transducers were installed below the surface of the centre span of each model. All transducers were temperature-compensated and factory-calibrated. Whilst these calibrations were accurate, the necessary cabling and signal conditioning of the transducer output rendered a slightly different system performance. As a consequence of this, the entire measurement system was calibrated for each model. The method used was to apply a time varying calibrated reference pressure to each of the model's pressure transducers in turn. Both reference and model transducer outputs were simultaneously recorded to yield a well defined calibration.

Instantaneous aerofoil incidence was determined by a linear angular potentiometer geared to the model's tubular support. The dynamic pressure in the wind tunnel working section was obtained from the difference between the static pressure in the working section, 1.2m upstream of the leading edge, and the static pressure in the settling chamber, as measured by a FURNESS FC012 electronic micromanometer.

A series of experiments was performed on the aerofoil by rotating it about the quarter chord axis under four types of motion : "static", oscillatory (sinusoidal) and constant pitch-rate "ramp" motion in both positive and negative directions. The majority of tests were performed at a Reynolds number of 1.5×10^6 (i.e. a Mach number of 0.11), but a small number were performed at Reynolds numbers of 1.0×10^6 and 2.0×10^6 (i.e. Mach numbers of 0.075 and 0.15 respectively).

Data were recorded over a range of incidence by sweeping through the thirty-two channels of the MINC multiplexed analogue-to-digital converter and, hence, logging pressure values at thirty locations plus dynamic pressure and angle of attack.

For a static experiment, the model's angle of attack was increased in steps of approximately 0.5^0 from the required starting incidence. After each increment in incidence, the flow was allowed to stabilise for a few seconds, and then each transducer's output was sampled 100 times and the mean value stored. After 64 sweeps of data were recorded, the model was returned to the starting incidence in steps of equal size to those on the upstroke.

The unsteady data which are employed in this analysis were recorded during ramp experiments in which the model's angle of attack was changed at a constant pitch-rate over a preset arc. The experiment was repeated so that five sets of 256 data sweeps were recorded. The reduced pitch-rate of these experiments varied over a range of values for which

$8 \times 10^{-5} < r < 5 \times 10^{-2}$ (i.e. $0.75^0 \text{s}^{-1} < \dot{\alpha} < 350^0 \text{s}^{-1}$).

All data collected by the data acquisition routines were stored in unformatted form on magnetic tape. A library of FORTRAN programs is available for the reduction and

presentation of the raw data by the MINC and DEC VAX 750 computers. By applying offsets, gains and calibrations to the raw data, the data reduction programs were used to convert the cycles of raw data into averaged or unaveraged non-dimensional pressure coefficients. The results were stored in unformatted form on the DEC VAX 750 in the University of Glasgow's aerofoil database.

3. DATA ANALYSIS TECHNIQUES

3.1 Established Techniques

In recent years, several methods have been employed to assess the timing of incipient dynamic stall. Some of these have involved the examination of airloads. Figure 5 illustrates the familiar characteristic time dependent airloads associated with dynamic stall and suggested indicators of the beginnings of that process. One such method was that of Beddoes [9], who, by examining the results of 150 test cases, concluded that, to a first order, each dynamic stall event is governed by a distinct universal non-dimensional time constant τ, regardless of the time history of the motion. In particular, he suggested that a time constant exists between the aerofoil pitching through the static stall incidence and experiencing both moment stall and maximum lift. The static stall incidence was defined as being the angle of attack at which there was an abrupt drop in the pitching moment curve.

Wilby [10] reasoned that aerofoil sections which exhibit, in oscillatory conditions, the ability to attain high incidence values without involving a break in pitching moment would be beneficial to helicopter rotor performance. In order to calculate the maximum incidence to which an aerofoil could be pitched without incurring moment stall, Wilby examined the data from a series of oscillatory tests for which the mean angle was steadily increased, whilst the amplitude and reduced frequency were fixed at 8.5^0 and 0.10 respectively. From those tests in which the mean angle was sufficiently large for a break in pitching moment to be detected, the difference ΔC_m between the minimum value of C_m and its unstalled value was calculated. These ΔC_m values were plotted against the maximum incidence for each cycle, and the intersection of the curve through these points with $\Delta C_m = 0$ was defined to be the critical incidence α_c. If this incidence is exceeded, a subsequent break in the pitching moment curve is unavoidable.

This critical incidence can only be calculated from oscillatory data. In order to investigate the dynamic overshoot of several new RAE blade sections, Wilby found it necessary, for ramp experiments, to define dynamic stall as occurring at the incidence at which the coefficient of pitching-moment had fallen by 0.05 below its maximum pre-stall value. This technique was also applied by Niven and Galbraith [11] when studying the unsteady behaviour of the NACA 23012A aerofoil.

When analysing Carta et al's [12] experimental data, Scruggs et al [13] defined dynamic stall onset as occurring at the incidence, on the upstroke, at which there is a sudden deviation in the gradient of the lift curve.

In the present procedure, the airloads were calculated by suitably integrating the recorded pressure coefficients around the aerofoil. As a consequence of.this, early indications of incipient stall may be disguised or hidden : during vortex initiation, it is likely that the formation of any localised disturbance within the boundary layer would be indicated immediately by the response of the local pressure coefficient, whereas the integrated airloads would de-sensitise the inception point. It was, therefore, decided that the onset of stall should be examined in relation to individual pressure traces.

A number of such methods have been employed by other researchers. Indeed, the stall criteria which are described above have been modified to include determination from local pressure values.

Wilby [14] employed ramp data, which were recorded at a freestream Mach number of

0.3, to investigate the effect of pitch-rate on an aerofoil's dynamic stall behaviour. He defined the stall incidence to be the angle of attack at which the pressure coefficient at 0.5% chord was at a minimum. It was observed that this was more clearly defined than a pitching moment break.

Beddoes [15] postulated that, under full unsteady conditions, dynamic stall is triggered at the leading edge. As a result, to calculate an idealised static stall incidence, he employed Evans and Mort's [16] correlation in which aerofoils are assumed to experience leading-edge stall by the reseparation mechanism. As explained in Section 5, this incidence is that at which the leading edge becomes critical, and is calculated theoretically by suppressing all trailing-edge separation. It follows that, for aerofoils which experience leading-edge stall, this incidence is very close to that of static stall. The dynamic stall onset incidence is then determined as the angle through which the aerofoil pitches after the expiry of the relevant non-dimensional time delay since pitching through the aforementioned equivalent static stall angle. This static stall incidence is used for low Mach numbers cases, in the latest version of Beddoes algorithm, which has been described by Leishman and Beddoes [17] and is discussed in Section 5 of this paper.

Daley and Jumper [18] performed a series of experiments in constant freesteam flow over a Reynolds number range for which $78300 < Re < 301000$. The aerofoil was pitched at a constant rate about its mid-chord axis. Stall was arbitrarily defined to occur at the incidence at which the boundary layer separated at the quarter-chord. Smoke-flow visualisation and pressure data were used to determine this location.

Lorber and Carta [19] performed, at a Mach number of 0.2, a series of experiments during which the aerofoil was pitched about its quarter-chord axis over a range of constant pitch-rates for which $0.001 < r < 0.02$. The vortex was monitored by means of the root-mean-square variation in unaveraged pressure readings.

From Carta's [20] display technique of pressure coefficient histories and from additional hot-film traces, McCroskey et al [2,3] found that, while a thin layer of reversed flow on the rear half of the aerofoil was moving forward, a major boundary layer disturbance and vortex erupted out of the leading edge region. Only later did these two distinct disturbances appear to meet at approximately mid-chord. These experiments revealed that the disturbances originated at approximately 25% chord and spread upstream and downstream from that general area.

Seto and Galbraith [21] found similar results when testing a NACA 23012 aerofoil in the manner described in Section 2. These results were supported by experiments which were performed by Seto [22] and Niven [5] with hot-film gauges. Based on these results, Seto and Galbraith established a criterion for indicating that the stall process had been initiated. This criterion has been employed in the present analysis to locate the lowest incidence at which it is observed that stall onset has occurred.

3.2 Data Analysis Technique in Present Use

A typical data set for a static test at a Reynolds number of 1.5×10^6 is illustrated in Figure 6(a). Other than a small area of hysteresis at the point of leading-edge reattachment, there was much similarity in the data recorded for both increasing and decreasing incidence. It may be seen that the leading-edge suction dropped a little at the stall incidence and, at an incidence greater than 20^0, collapsed.

At low pitch rates the overall qualitative characteristics of the pressure profile history were unaltered, albeit significant lift and moment overshoot were evident (Figure 6(b)). This response is labelled "quasi-static", and the limit to this regime was observed to be at a reduced pitch-rate of 0.01. For values in excess of this (Figure 6(c)), the upper surface pressure distribution revealed evidence of a vortex. The suction peak collapsed soon after vortex initiation and the gradient of the C_n versus α graph was reduced. There was a subsequent dynamic overshoot of C_n and C_m. These effects were enhanced by increasing the pitch-rate

and this characteristic response is associated with "Dynamic" stall.

Figure 7 illustrates, in the manner of Carta [20], the variation with incidence of the pressure coefficient at each transducer location over the upper surface. The first indication that the dynamic stall vortex had been initiated was found to be when an abrupt deviation in the gradient of one of the C_p traces was observed. The incidence at which this deviation in the C_p gradient occurred was defined as being the incidence of intersection between two straight lines, which had been determined from linear regression, through data points before and after stall onset (see Figure 8). The presence of this C_p deviation distinguishes dynamic stall from quasi-static stall. The fact that this deviation is initially so small reveals why it is regarded as being more accurate to examine individual pressure traces rather than integrated airloads. Hereafter this response will be referred to as the C_p deviation.

The transducer location of the first C_p deviation was found to vary with aerofoil. Over the range of aerofoils for which results are discussed in this paper, this location was found to be between 25% and 60% chord. For the NACA 23012 aerofoil, the earliest deviation in the C_p trace occurred at 34% chord.

Illustrated in Figure 9 is the variation of the incidence of first deviation in C_p trace with reduced pitch-rate for the NACA 23012C aerofoil. This C_p deviation, and its associated incidence, is the earliest indication which can be observed from the examination of the pressure histories using the current procedures and definitions of incipient Dynamic Stall. Evidence discussed in Section 5 shows that this is not the stall trigger, but it is the earliest indication that can be observed from experimental data based on pressure readings. A comparison between this lowest angle of attack at which the vortex is detected and the incidence of peak suction collapse in Figure 9 confirms that the former does occur first. However, in the quasi-static regime, no vortex is formed and so it is necessary to determine the earliest indication of stall by a different method. In this case, the earliest indication was taken to be the collapse of the leading-edge peak suction.

In the dynamic regime, the variation of the earliest observed stall incidence with pitch rate is approximately linear. However, as can be seen from Figure 10, the gradient of the best least-squares straight line through these points varies significantly over the range of the test aerofoils considered in this paper. The aim is to find some method by which all these lines may be represented by a single equation. This must involve using parameters which are unique to each aerofoil. As will be seen, these parameters are yielded by the data which were obtained during static experiments.

It should be stressed that the analysis which has been discussed above has only been performed on aerofoils experiencing trailing-edge stall at low Mach numbers : the highest recorded local Mach number was less than 0.8. Therefore, these results may only be typical of such cases.

4. A CORRELATION INDICATING INCIPIENT DYNAMIC STALL

4.1. Physical Reasoning

With the aid of a numerical boundary layer model, Scruggs et al [13] demonstrated that there was a high degree of correlation between the incidence at which significant flow reversal reached the 50% chord location and the experimentally-measured incidence of dynamic stall onset. This model also predicted that, with increasing pitch-rate, the extent of the delay in flow reversal increases and the subsequent forward movement of the flow-reversal point becomes progressively more rapid. However, it was stressed that this analysis did not imply that dynamic stall is simply the result of this forward movement of the flow-reversal point.

Water tunnel experiments by McAlister and Carr [23] found that, prior to vortex formation, a region of reversed flow momentarily appeared over the entire upper surface without any appreciable disturbance to the viscous-invisid boundary. McCroskey et al [2,3]

observed that for aerofoils which displayed a gradual trailing-edge static stall, vortex initiation was preceded by a gradual forward movement of flow reversal in a thin layer at the bottom of the boundary layer. This behaviour has been described as a "tongue of reversed flow" since it was found that no upper surface pressure divergence, indicating possible boundary-layer separation, was observed. Carr et al [1] also found that the occurrence of surface flow reversals over the rear portion of the aerofoil were not necessarily synonymous with flow breakdown outside the boundary layer.

At the University of Glasgow, correlations between pressure data and hot-film traces have been carried out [5] for both the NACA 23012 and 23012A aerofoils. These data have also indicated that flow reversals may penetrate upstream to the 30% chord region prior to vortex formation.

These results raise the interesting question: are these flow reversals a necessary precursor to vortex inception, and, if so, is their behaviour dependent on the aerofoils static trailing-edge separation characteristics? One method of investigating this phenomenon would be to correlate the incidence at which vortex initiation is observed against a designated parameter representing the aerofoil's static trailing-edge separation characteristics. The results of McCroskey et al [3] imply that the incidence at which dynamic stall onset occurred was related to the abruptness of the aerofoils static trailing-edge separation, and therefore it seemed reasonable to look for a parameter which describes this behaviour.

4.2 The Correlation

An approximation to the location of boundary layer separation for an aerofoil experiencing trailing-edge separation has been described by Beddoes [24]. The variation of the separation point with incidence was modelled by two exponential equations which coincided at the 70% chord location. In forming the present correlation it was decided [6] that these equations should be generalised to the form

$$f = f_{max} + K_1 \exp \left((\alpha - \alpha_1) / S_1 \right), \; \alpha \le \alpha_1 \tag{1a}$$

$$f = f_{min} + K_2 \exp \left((\alpha_1 - \alpha) / S_2 \right), \; \alpha \ge \alpha_1, \tag{1b}$$

where α represents the angle of attack and f represents the separation point in the form of x/c. The remaining seven coefficients are constant for a particular aerofoil and Reynolds number under static conditions. An algorithm for approximating these constants for any set of data points $\{(\alpha, f)\}$ has been coded, and the resulting separation curves for the seven aerofoils are illustrated in Figure 11.

The larger range of values for f, including the region of the more sudden forward movement of the separation point, is included in Equation (1b). It follows that, at this part of the separation process,

$$df/d\alpha = -S_2^{-1} K_2 \exp \left((\alpha_1 - \alpha) / S_2 \right)$$
$$= -S_2^{-1} (f - f_{min}).$$

The constant f_{min} represents the location of bluff body separation (i.e. fully separated flow), and is approximately equal for each aerofoil ($0 < f_{min} < 0.0025$). Therefore, for any given value of f in the range of abrupt separation and at the 50% chord location which Scruggs et al [13] examined when comparing aerofoils' separation characteristics, the rate of change of separation point with incidence is approximately proportional to S_2^{-1}. From the argument stated above, it would, therefore, seem that the statically-derived coefficient S_2 would be a suitable parameter to use when examining the influence of trailing-edge separation on vortex inception. If this parameter does influence the formation of the vortex, it should be possible, in the light of what has been previously discussed, to use it when representing, in the form of single equation for all seven aerofoils, the incidence of the earliest indication of the occurrence

stall onset.

In the fully dynamic stall regime, the angle of attack α_{ds} at which it is first observed that stall onset has occurred varies with pitch-rate r in the form

$$\alpha_{ds} = m_1 r + c_1, \tag{2}$$

where m_1 and c_1 represent constants for a particular aerofoil. If the rate of separation influences the formation of the vortex, then it is possible that

$$m_1 = F_1(S_2) \, m_2,$$

where m_2 is a constant for all aerofoils and $F_1(S_2)$ is a function of S_2 and, hence, of aerofoil. By correlating m_1 against S_2, and with the intention that the function should be as simple as possible, it was decided that $F_1(S_2)$ should be of the form $S_2{}^i$, where i is a constant for all aerofoils. For each of a number of values of i, the set of values $\{m_1 S_2{}^{-i}\}$ over the range of aerofoils at a Reynolds number of approximately 1.5×10^6 was statistically examined, and the most suitable value of i was determined. It was discovered that $i = {}^1/_3$ and $i = {}^1/_4$ resulted in an accurate correlation.

Because the static stall characteristic can be regarded as the characteristic of a ramp test with zero pitch-rate, it seemed natural to consider the static stall incidence α_{ss} as the aerofoil-dependent static parameter for the offset value c_1 in equation (2). Regardless of how the static stall angle is defined, it is of the same order as c_1 and so the logical substitution seemed to be

$$c_1 = c_2 \, \alpha_{ss} + c_3,$$

where c_2 and c_3 are constants for all aerofoils. This was supported by correlating c_1 against α_{ss}. It follows that α_{ds} can be represented in the form

$$\alpha_{ds} = A + B \, \alpha_{ss} + C.S_2{}^i r, \tag{3}$$

and values for A, B and C must be calculated.

In the dynamic stall regime for each aerofoil, the gradient and offset of the linear representation for the variation of α_{ds} with pitch-rate were used in determining the form of Equation (3). The gradient m_1 and offset c_1 in Equation (2) were calculated by least-squares regression through a set of data points for each individual aerofoil. These values in themselves, therefore, contain errors. In order to minimise these errors, once the basic form of the equation was known, all further curve fitting procedures were performed on all data points as one set, regardless of aerofoil (of course, the values of S_2 and α_{ss} were still dependent on aerofoil). For this purpose, an algorithm was coded to perform least-squares linear regression in two variables on the data points at a Reynolds number of approximately 1.5×10^6. These two variables were $S_2{}^i r$ and α_{ss}. For a given value of i, the algorithm calculated A, B,C and the least-squares error. Repeating the process with different values of i and comparing the resulting error values provided a suitable equation.

Initially, α_{ss} was regarded as being the first incidence at which the normal force slope became zero. However, although a good correlation was achieved for each family of aerofoils, the NACA 0021 data did not fit when correlating for all seven aerofoils. The incidence of

pitching-moment break was then substituted and much better agreement resulted. This definition of the static stall incidence was employed in all further modifications of the correlation.

The correlation program yielded the most suitable results when i was assigned the value $^1/_4$. Equation (3) is the equation of a plane in three dimensions. Any qualitative comparison of the original set of data points to those predicted by the equation with the aid of a three-dimensional diagram would be very difficult. Therefore, it was decided to illustrate the correlation as in Figure 12, by means of a two-dimensional graph with the axes labelled $S_2{}^i r$ and $(\alpha_{ds} - B\ \alpha_{ss})$.

The resulting correlation was reasonable, but could have been more accurate : the general trend was not quite linear. In addition, it was decided that data points which resulted from quasi-static experiments should be included. It was discovered that the inclusion of a square-root term was a simple and accurate modification, resulting in an equation of the form

$$\alpha_{ds} = A + B\ \alpha_{ss} + C.\ S_2{}^i r + D(\ S_2{}^i r)^{1/2}. \tag{4}$$

The original program was modified to implement this change and a good correlation was achieved. This is illustrated in Figure 13, in which a square-root scale was used on the $S_2{}^i r$ axis so that the comparison in the quasi-static region could be made more easily.

All the data used to form Equations (3) and (4) were recorded at a Reynolds number of approximately 1.5×10^6. The next modification to the algorithm was the consequence of an attempt to include points at other Reynolds numbers. It was hoped that the only necessary change would be to determine α_{ss} and S_2 at each Reynolds number. However, examination of the graphs which resulted from this modification indicated that the power to which S_2 is raised should be a function of Reynolds number, and that Equation (4) should be modified to the form

$$\alpha_{ds} = A + B\ \alpha_{ss} + C.\ S_2{}^R j r + D\ (S_2{}^R j r)^{1/2}, \tag{5}$$

where $R = Re \times 10^{-6}$ and j is a constant for all aerofoils. The final correlation is illustrated in Figure 14, and is compared with the data points which were recorded for the NACA 23012C in Figure 15. In this Figure the correlation is compared to two sets of data points : data determined at 0% chord and data determined at 27% chord. In addition, in the quasi-static regime, the incidence at which the peak suction collapsed at 27% chord is plotted. This is the lowest incidence at which there is a deviation in C_p gradient at such pitch-rates. As would be expected, in the quasi-static regime, it can be seen that the correlation refers to the peak suction collapse at 0% chord and, in the dynamic regime, to the C_p deviation 27% chord.

McCroskey et al [2] found that, regardless of behaviour at low Mach number or in the quasi-static regime, as the freestream Mach number was increased, each aerofoil which they tested tended to exhibit characteristics typical of unsteady leading-edge stall. It is, therefore, noted that the present correlation is restricted not only to aerofoils which experience trailing-edge separation but also to test conditions in the low Mach number regime (i.e. $M_\infty < 0.2$).

5. MODELLING

5.1 The Model

At present, detailed comparisons have been made between a particular dynamic stall model (Leishman and Beddoes [17]) and the experimental data specific to the NACA 23012C aerofoil. A version of this model has been coded at Glasgow University from the relevant equations cited in Leishman [25]. In order to make these comparisons meaningful, a brief

description of the model elements relevant to vortex initiation is now given.

A prerequisite to any unsteady aerodynamic model is the ability to accurately represent the aerofoil's attached flow behaviour. It is possible to formulate this problem in terms of the unsteady response to a step change in forcing - the indicial response (Lomax [26]). These solutions can subsequently be manipulated by superposition, with the aid of Duhamel's integral (Tobak [27]), to obtain the cumulative response to an arbitrary forcing. Efficient numerical algorithms for this superposition procedure have been developed for use in discrete time analyses, and have been outlined by Beddoes [28].

A fundamental aspect in modelling dynamic stall is the determination of the vortex initiation incidence. In 1978, Beddoes [15] showed that it was possible to use a leading-edge velocity criterion to predict the onset of dynamic stall. For a set of aerofoils which exhibited static leading-edge stall by the reseparation process, Evans and Mort [16] computed the velocity distribution and obtained a correlation between the maximum obtainable peak velocity U_{pcrit} and a parameter idealising the adjacent adverse pressure gradient. For many practical aerofoils, maximum lift is limited by trailing-edge separation under static conditions and so the leading edge never achieves the high local velocity appropriate to the above study. Under dynamic conditions, however, trailing-edge separation is suppressed (Carr et al [1]) and so, depending on the rate of increase of incidence, the leading edge may become critical according to the Evans and Mort correlation. Beddoes [15] illustrated theoretically that, for practical applications, the variation in U_{pcrit} with pitch rate was small and, therefore, it was possible to assume that U_{pcrit} was constant for a given aerofoil at a given Mach number. Combining this result with the postulation that only the peak pressures at the aerofoil leading edge or ahead of the shock wave were important, allowed Beddoes to extend the Evans and Mort static separation criterion into the dynamic regime.

For practical purposes, it was determined by Beddoes [24], that a lift value associated with the critical angle of incidence, which invoked the leading-edge pressure criterion, was appropriate to denote dynamic stall onset. Thus, using the leading-edge pressure criterion at low Mach numbers and a shock reversal condition at high Mach numbers, a generalised criterion was derived for the onset of leading-edge or shock induced stall in terms of a critical normal force C_{n1}. From unsteady aerofoil tests, it has been observed that, under nominally attached flow conditions, there is a lag in the leading-edge pressures with respect to the instantaneous normal force. Beddoes illustrated that the simplest representation of this behaviour was via a first order lag with a Mach number-dependent time constant T_p. This made it possible to relate the pressure in the unsteady flow to the static relation by applying a lag to the value of the normal force, producing a value C_n'. In the Laplace domain, this can be written as:

$$C_n^1(p) / C_n(p) = 1 / (1+T_p p)$$

When the values of the unsteady pressures are compensated using this approach, it is apparent, from Figure 16, that the pressures correlate with the static behaviour. Leishman and Beddoes [17] demonstrated that the same form of compensation applies to other Mach numbers, and the values of T_p obtained for a NACA 0012 aerofoil for a range of Mach numbers are shown in Table 1. Thus, in terms of $C_n'(t)$, initiation of the dynamic stall process will occur at the incidence at which $C_n'(t)$ is equal to the critical C_{n1} value appropriate to the given freestream Mach number.

5.2 Comparison with Correlation

The following procedure was adopted to calculate the necessary input parameters required by the dynamic stall model. The theoretical leading-edge velocity distribution appropriate to the NACA 23012C was computed through a range of incidence values using a vortex panel method with wake modelling. At each incidence the trailing-edge separation point was varied until the appropriate value of lift, based on the experimental lift-curve slope and zero-lift angle, was achieved, i.e. the Kutta condition was ignored. This procedure was

continued until the Evans and Mort criterion for leading-edge flow breakdown was satisfied, thus giving values for both the critical normal force C_{nl} and the accompanying critical pressure coefficient C_{pcrit} at the 0.25% chord position. Based on comparisons between the pressure response at the 0.25% chord obtained during static, ramp and oscillatory tests, a value of 1.3 was estimated for T_p (Figure 17). A coded version of the Beddoes model is linked directly with the database to allow comparisons to be made with the dynamic stall test data. The model is therefore driven by the angular motion array from the test data, which can be passed through a filtering routine if required. The remaining input parameters to the model are derived from the static characteristics of the aerofoil in question.

Figure 18 illustrates the comparison between experimental data for the NACA 23012C, the Beddoes prediction appropriate to this aerofoil, and the generalised correlation. Initially it would seem that there is no agreement between the prediction and the experimental data. However, a consideration should be made of the particular methods adopted by both the data analysis technique and the prediction to define the incidence at which vortex initiation occurs. Whereas the prediction flags vortex initiation when the leading-edge pressure distribution becomes critical, the data analysis technique can only consider the first observable sign that dynamic stall has occurred which, as detailed in Section 3, was a divergence in local pressure coefficient at a particular chordwise position. It has been shown [29] that this finding is significant, because it suggests that, if the leading-edge velocity distribution is assumed to trigger the initial boundary-layer breakdown, there exists a finite time within which this region of disturbed flow develops into a vortex structure, causing a distortion of the local chordwise pressure distribution. To a first order, a non-dimensional time delay τ_{vb} between these two events can be calculated, and the value obtained for the NACA 23012C was approximately 1.7. Figure 19 displays the upper surface pressure-time histories obtained for the NACA 23012C during a ramp test at a reduced pitch rate of 0.021. The non-dimensional time delay of 1.7 between the critical pressure at the 0.25% chord and the suction roll-up at the 27% chord is clearly shown.

On consideration of vortex formation, it may be speculated that the process consists of three phases: vortex initiation, incipient growth and subsequent convection downstream. The formation of the stall vortex is an apparent consequence of the boundary-layer response to the chordwise velocity distribution induced by the imposed incidence variation. Therefore, vortex inception may be expected to display a dependency on not only the motion but also the same parameters which influence boundary-layer development, i.e. aerofoil geometry, Reynolds number, and Mach number. Also, when considering the unsteady response of the boundary layer, its behaviour is governed by the relative magnitudes of the temporal and spatial velocity gradients. This relationship is governed by both the section geometry and the degree of unsteadiness imposed on the aerofoil by the forcing function. The initial development of the dynamic stall vortex may be expected to be dependent on the development of the necessary conditions for vortex growth in the region of localised boundary-layer breakdown. The manner in which this is achieved may also be related to the geometry of the aerofoil. McCroskey et al [3] noted that, for the NACA 0012 aerofoil, the shed vortex appeared to be fed its initial vorticity by the abrupt unsteady separation of the turbulent boundary layer over the forward portion of the aerofoil. It was also observed by Niven [5] that, as the vortex began to form, the magnitude of the reversed flow velocity increased. For trailing-edge stalling aerofoils, perhaps vortex growth is assisted by fluid supplied by a thin layer of reversed flow at the bottom of the boundary layer penetrating upstream. If this is the case, and this behaviour is related to the aerofoil's static separation characteristics, then this may explain why a relationship exists between the C_p deviations and the S_2 parameter.

6. CONCLUSIONS

Over a range of pitch-rates, the pressure coefficient traces from seven aerofoils have been examined. It has thus been possible to determine the angle of attack at which the first indication of incipient dynamic stall can be observed from pressure-based data. It is possible to predict this incidence from the static characteristics of each aerofoil at a particular Reynolds number. The necessary "statically-derived" parameters are the incidence of pitching-moment stall and an additional parameter representing the incidence locus of the trailing-edge separation

location.

A comparison has been made between the dynamic stall onset incidence as predicted from both an indicial-based dynamic stall model and the present correlation. In agreement with previous observations, this work has indicated that, if the leading-edge velocity distribution is assumed to trigger the initial boundary-layer breakdown, there exists a finite time within which this region of disturbed flow develops into a vortex structure causing a distortion of the local chordwise pressure distribution.

ACKNOWLEDGEMENTS

REFERENCES

1) L. W. Carr, et al., Analysis of the Development of Dynamic Stall based on Oscillating Airfoil Experiments, NASA TN D-8382, Jan. 1977.

2) W. J. McCroskey, et al., Dynamic Stall on Advanced Airfoil Sections, J. American Helicopter Society, Vol. 13, pp40-50, July 1981.

3) W. J. McCroskey, et al., Dynamic Stall Experiments on Oscillating Airfoils, AIAA Journal, Vol. 14, No. 1, pp57-63, Jan. 1976

4) W. H. Young. Jr., Fluid Mechanics Mechanisms in the Stall Process for Helicopters, NASA TM-81956, Mar. 1981.

5) A. J. Niven, An Experimental Investigation into the Influence of Trailing-Edge Separation on an Aerofoils Dynamic Stall Performance, Ph. D Dissertation, University of Glasgow, Scotland, 1988.

6) M. W. Gracey, The Design and Low Mach Number Wind-tunnel Performance of a Modified NACA 23012 Aerofoil, with an Investigation of Dynamic Stall Onset. Ph. D Dissertation, University of Glasgow, Scotland. (In preparation.)

7) D.G.F. Herring and R.A.McD. Galbraith, The Collected Data for Tests on a NACA 23012B Aerofoil. Volume 1: Description, Pressure data of Static Tests with Oil-Flow Visualisation, Glasgow University Aero Rpt. 8808, June 1988.

8) J. G. Leishman, Contributions to the Experimental Investigation and Analysis of Aerofoil Dynamic Stall, Ph. D Dissertation, University of Glasgow, Scotland, 1984.

9) T. S. Beddoes, A Synthesis of Unsteady Aerodynamic Effects including Stall Hysteresis, Vertica, Vol 1, pp113-123, 1976.

10) P. G. Wilby, The Aerodynamic Characteristics of some New RAE Blade Sections, and their Potential Influence on Rotor Performance, Vertica, Vol. 4, pp121-133, 1980.

11) A. J. Niven and R. A. McD. Galbraith, The Effect of Pitch Rate on the Dynamic Stall of a Modified NACA 23012 Aerofoil and Comparisons with the Unmodified Case, Vertica, Vol. 11, No. 4, pp751-759, 1987.

12) F. O. Carta, et al., Investigation of Airfoil Dynamic Stall and its Influence on Helicopter Control Loads, U.S.A.A.M.R.D.L. Technical Rpt. No. 72-51, Sept. 1972.

13) R. M. Scruggs, et al., Analysis of Dynamic Stall using Unsteady Boundary-Layer Theory, NASA CR-2462, Oct. 1974.

14) P. G. Wilby, An Experimental Investigation of the Influence of a Range of Aerofoil Design Features on Dynamic Stall Onset, Paper presented at 10th European Rotorcraft Forum, No. 2, Aug. 28-31 1984.

15) T. S. Beddoes, Onset of Leading-Edge Separation Effects under Dynamic Conditions and Low Mach Number, Paper presented at American Helicopter Society 34th. Annual Forum, Washington, May 1978.

16) W. T. Evans and K. W. Mort, Analysis of Computed Flow Separation Parameters for a set of Sudden Stalls in Low Speed Two-Dimensional Flow, NASA TND-85, 1959.

17) J. G. Leishman and T. S. Beddoes, A Semi-Empirical Model for Dynamic Stall, J. American Helicopter Society, Vol. 34, No. 3, July 1989.

18) D. C. Daley and E. J. Jumper, Experimental Investigation of Dynamic Stall for a Pitching Airfoil, J. Aircraft, Vol. 21, No. 10, Oct. 1984.

19) P. F. Lorber and F. O. Carta, Airfoil Dynamic Stall at Constant Pitch Rate and High Reynolds Number, Paper presented at AIAA 19th Fluid Dynamics, Plasma Dynamics and Lasers Conference, No. AIAA-87-1329, Hawaii, Jun. 8-10 1987.

20) F. O. Carta, Analysis of Oscillatory Pressure Data including Dynamic Stall Effects, NASA CR-2394, 1974.

21) L. Y. Seto and R. A. McD. Galbraith, The Effect of Pitch Rate on the Dynamic Stall of a NACA 23012 Aerofoil, Paper presented at 11th European Rotorcraft Forum, No. 34, London, Sept. 10-13 1985.

22) L. Y. Seto, An Experimental Investigation of Low Speed Dynamic Stall and Reattachment of the NACA 23012 Aerofoil under Constant Pitch Motion, Ph. D Dissertation, University of Glasgow, Scotland, 1988.

23) K. W. McAlister and L.W. Carr, Dynamic Stall Experiments on the NACA 0012 Airfoil, NASA TP-1100, Jan. 1978.

24) T. S. Beddoes, Representation of Airfoil Behaviour, Vertica, Vol. 7, No. 2 pp183-197, 1983.

25) J. G. Leishman, Practical Modelling of Unsteady Airfoil Behaviour in Nominally Attached Two-Dimensional Compressible Flow, University of Maryland Rpt. UM-AERO-87-6, April 1987.

26) H. Lomax, et al., Two- and Three-Dimensional Unsteady Lift Problems in High Speed Flight, NACA Rpt. 1077, 1952

27) M. Tobak, On the use of the Indicial Function Concept in the Analysis of Unsteady Motions of Wings and Wing-Tail Combinations, NACA Rpt. 1188, 1954.

28) T. S. Beddoes, Practical Computation of Unsteady Lift, Vertica, Vol. 8, No. 1, pp55-71, 1984.

29) A. J. Niven, Preliminary Comparisons between a Semi-Empirical Dynamic Stall Model and Unsteady Aerodynamic Data obtained from Low Mach Number Wind-tunnel Tests, Glasgow University Aero. Rpt. (In preparation)

NACA 0012	
M_∞	T_p
0·30	1·7
0·40	1·8
0·50	2·0
0·60	2·5
0·70	3·0
0·75	3·3
0·80	4·3

Table 1   Variation in Tp with Mach Number
(from Leishman and Beddoes [17])
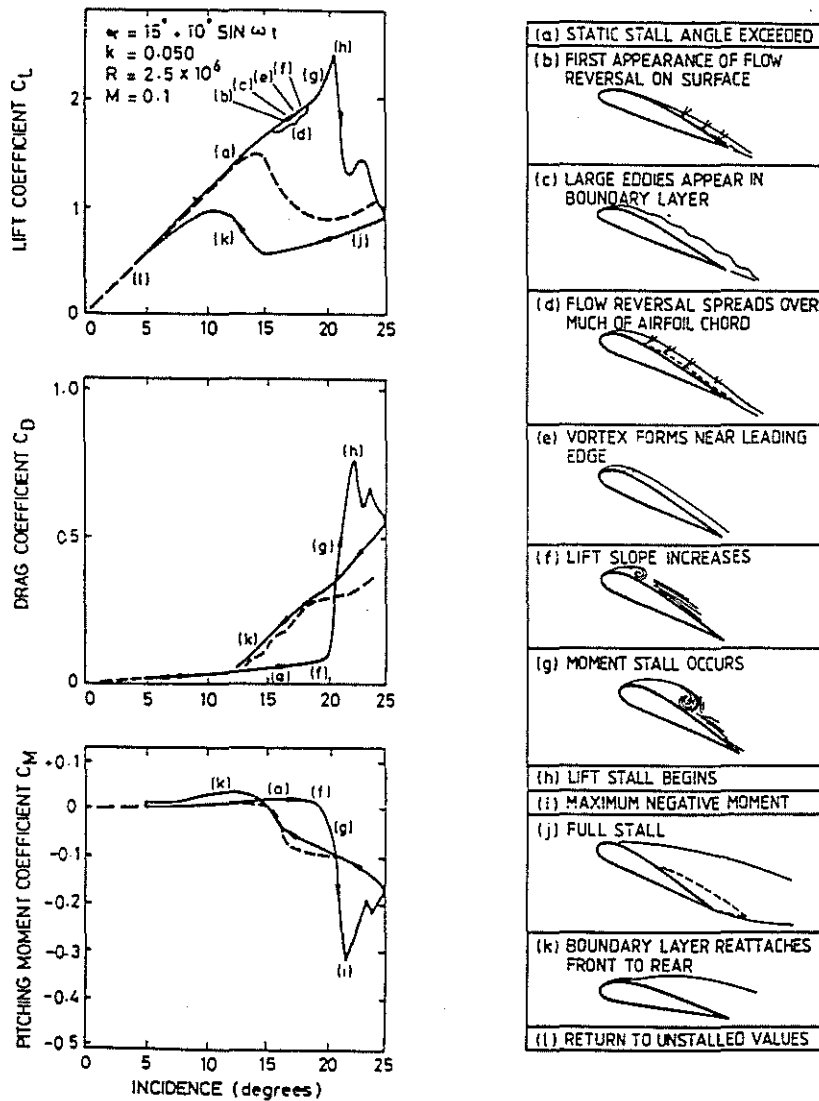
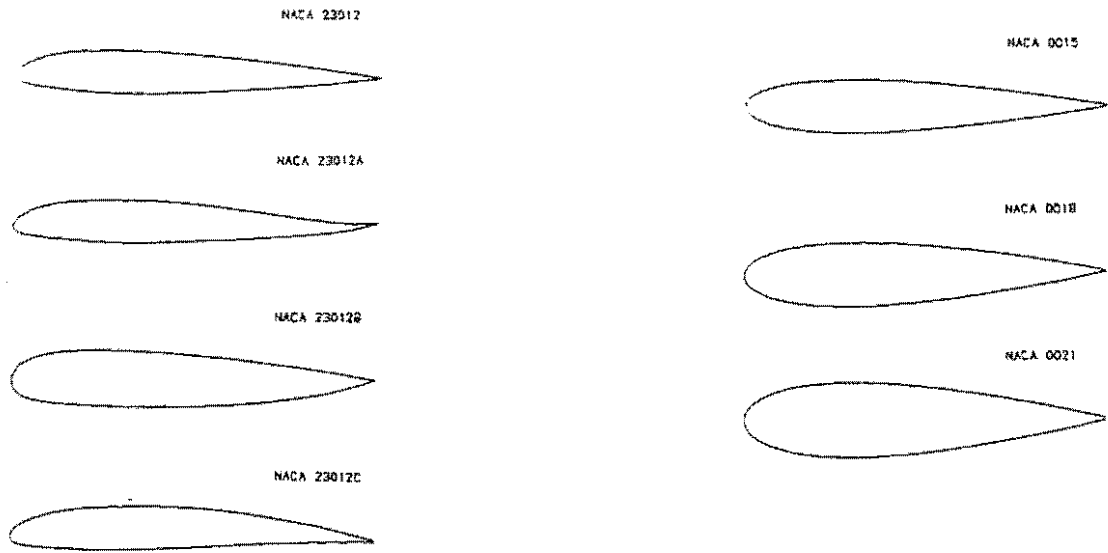Figure 1   Dynamic Stall Events on a NACA 0012 Aerofoil
(from Carr et al [1])

NACA 23012

NACA 23012A

NACA 230128

NACA 23012C

NACA 0015

NACA 0018

NACA 0021

Figure 2   Seven Aerofoils Tested at Glasgow University

NACA 23012C AEROFOIL

PRESSURE IN
SETTLING CHAMBER

PRESSURE IN
WORKING SECTION

MICRO-
MANOMETER

PIVOT

ANGULAR
DISPLACEMENT
TRANSDUCER

HYDRAULIC
ACTUATOR

PRESSURE
SIGNALS

30 SIGNAL
CONDITIONERS

31 SAMPLE & HOLD
CIRCUITS

JUNCTION
CIRCUIT

ST2

DYEXX10H

HYDRAULIC
POWER
PACK

D/A
CONVERTER

REAL-
TIME
CLOCK

A/D
CONVERTER

32 CH.
MULTI-
PLEXER

HYDRAULIC
CONTROLLER

MINC BUS

DEC
MINC - 11
MICROCOMPUTER

DRIVE
MSO:

DRIVE
DYO:

DRIVE
DLO:

LD1:

BBC
MICRO

D/A
CONVERTER

MAGNETIC
TAPE

DRIVE
DY1:

LD2:

FUNCTION GENERATOR

PRINT-
GRAPHICS

FLOPPY
DISC
SYSTEM

WINCHESTER
DISC SYSTEM

LD4:

DEC VT-105
TERMINAL

DEC VT-100
WITH VT640
GRAPHICS

ANADEX PRINTER

Figure 3   Schematic Arrangement of Data Acquisition
and Control System
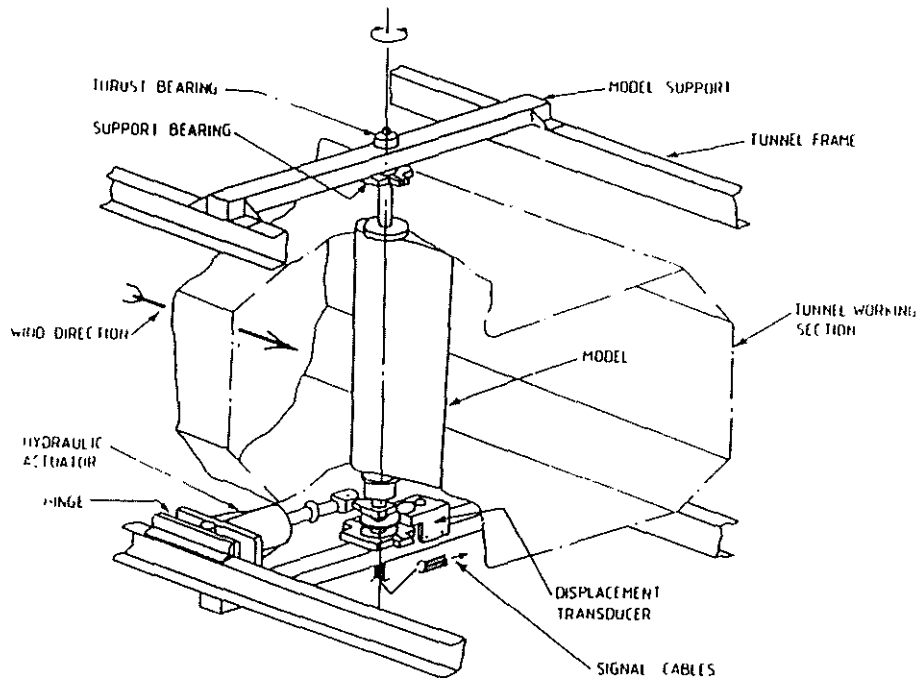
Figure 4   Wind Tunnel Working Section with Unsteady Aerofoil Test Apparatus
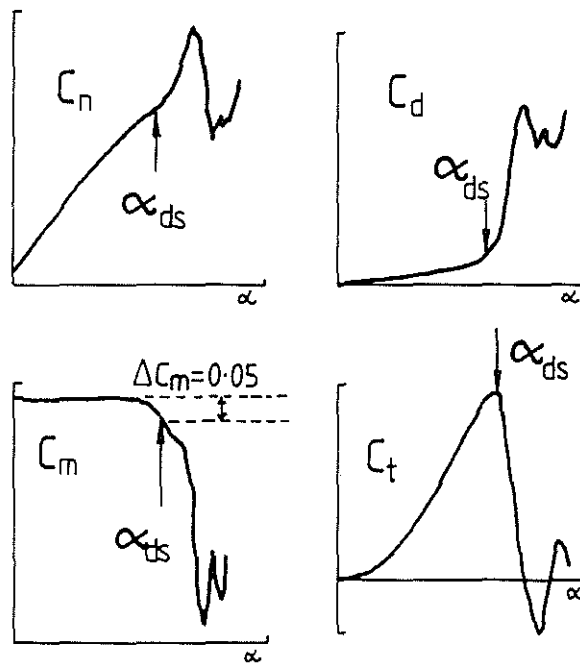
Figure 5   Definitions of Dynamic Stall Onset Incidence from Airloads (Low Mach Number)

(a) Static

(b) Ramp, r = 0.0017 (Quasi-static)

(c) Ramp, r = 0.021 (Dynamic)
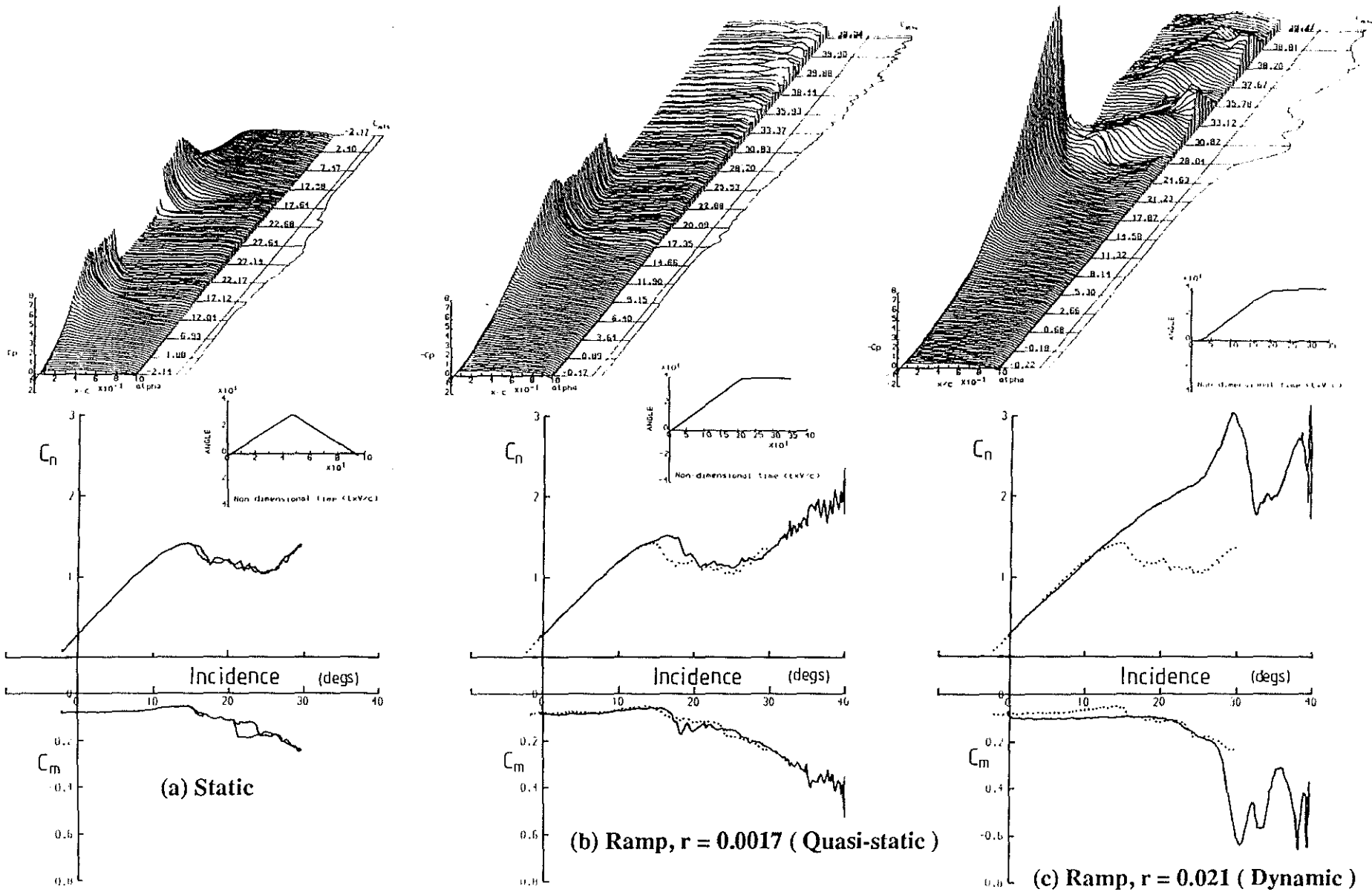
Figure 6   NACA 23012C Aerodynamic Data, Re = 1.5 x 10^6, M = 0.11
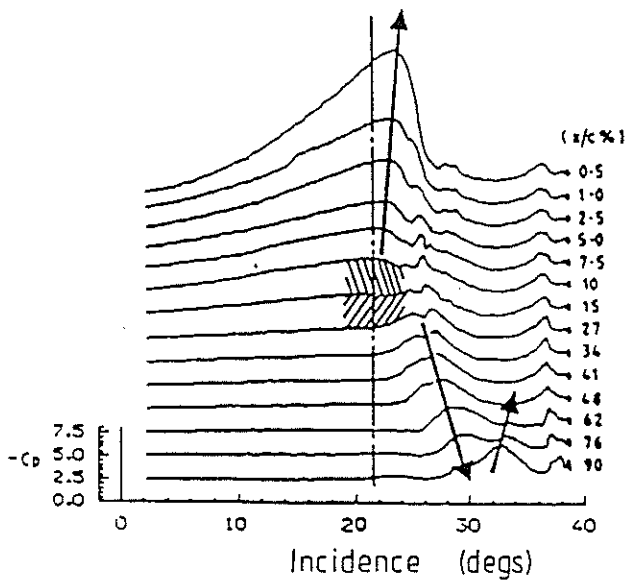
Figure 7   Upper Surface Pressure Variation for the
NACA 23012, Ramp Test r = 0.02
$Re = 1.5 \times 10^6$, $M_\infty = 0.11$
(from Seto and Galbraith[21])
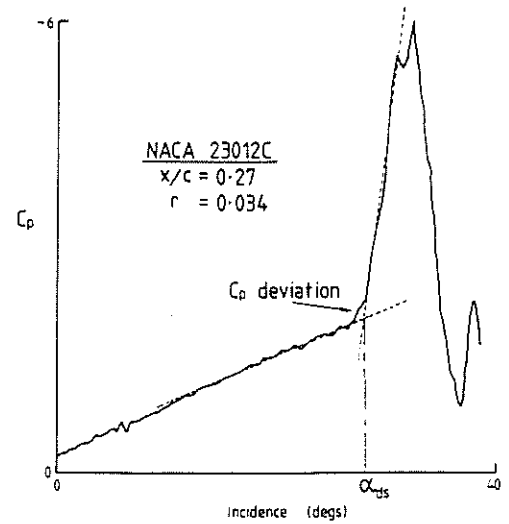
Figure 8   Defined Incidence of Dynamic
Onset from Pressure Trace
$Re = 1.5 \times 10^6$, $M_\infty = 0.11$
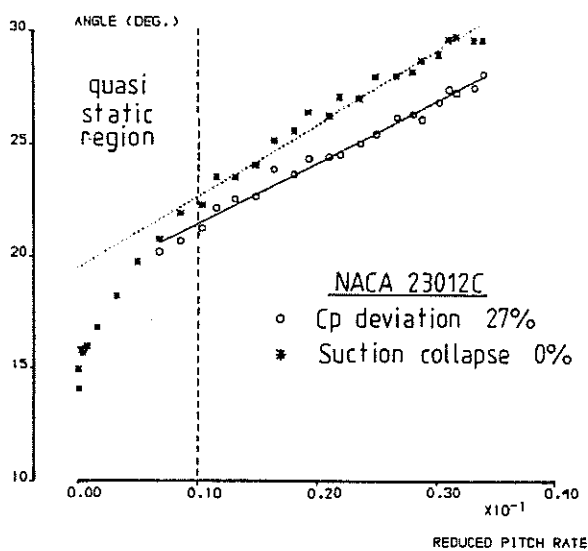
Figure 9   Variation of Defined Dynamic Stall
Onset Incidence with Reduced Pitch
Rate $Re = 1.5 \times 10^6$, $M_\infty = 0.11$
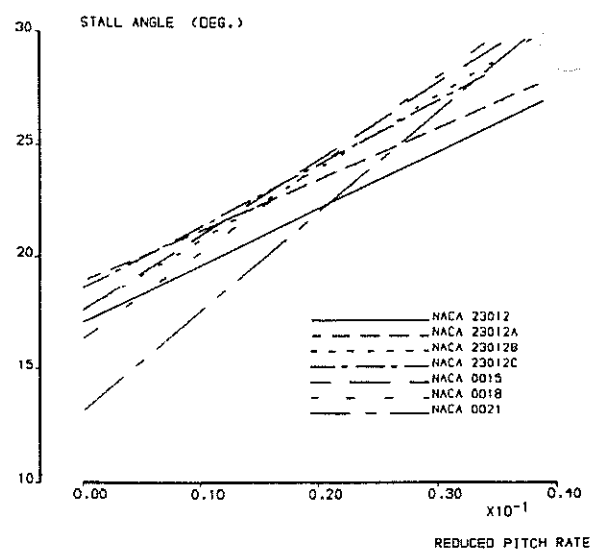
Figure 10   Variation of Defined Dynamic Stall Ons‹
Incidence with Reduced Pitch Rate for
Seven Aerofoils, $Re = 1.5 \times 10^6$, $M_\infty = 0.$
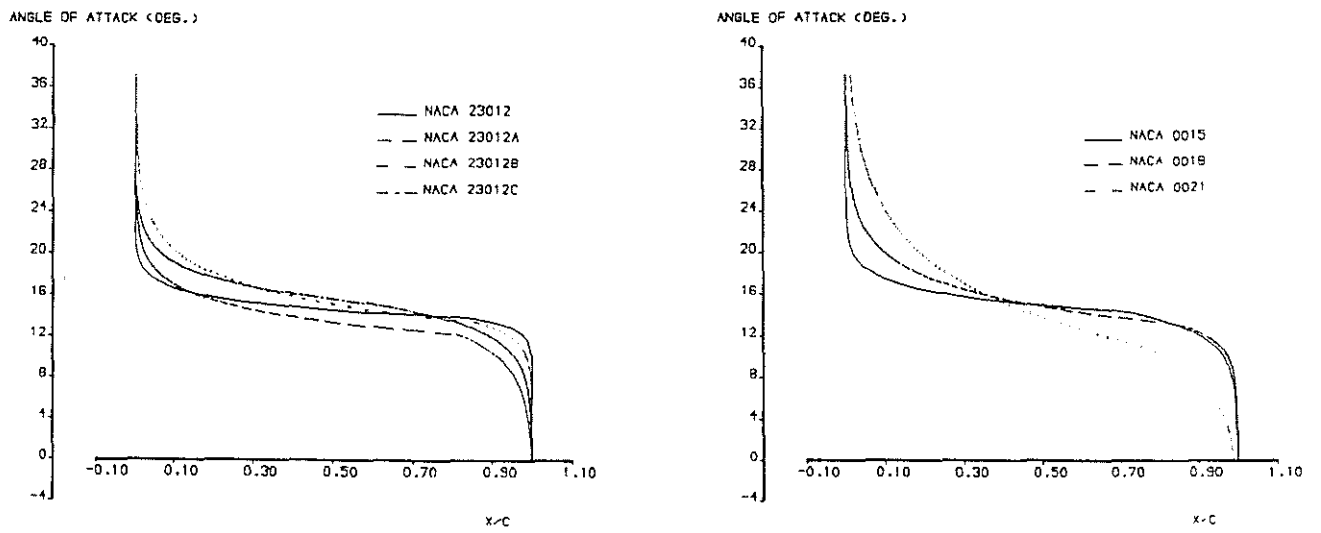
Figure 11   Static Trailing-Edge Separation Characteristics
$$Re = 1.5 \times 10^6, M_\infty = 0.11$$
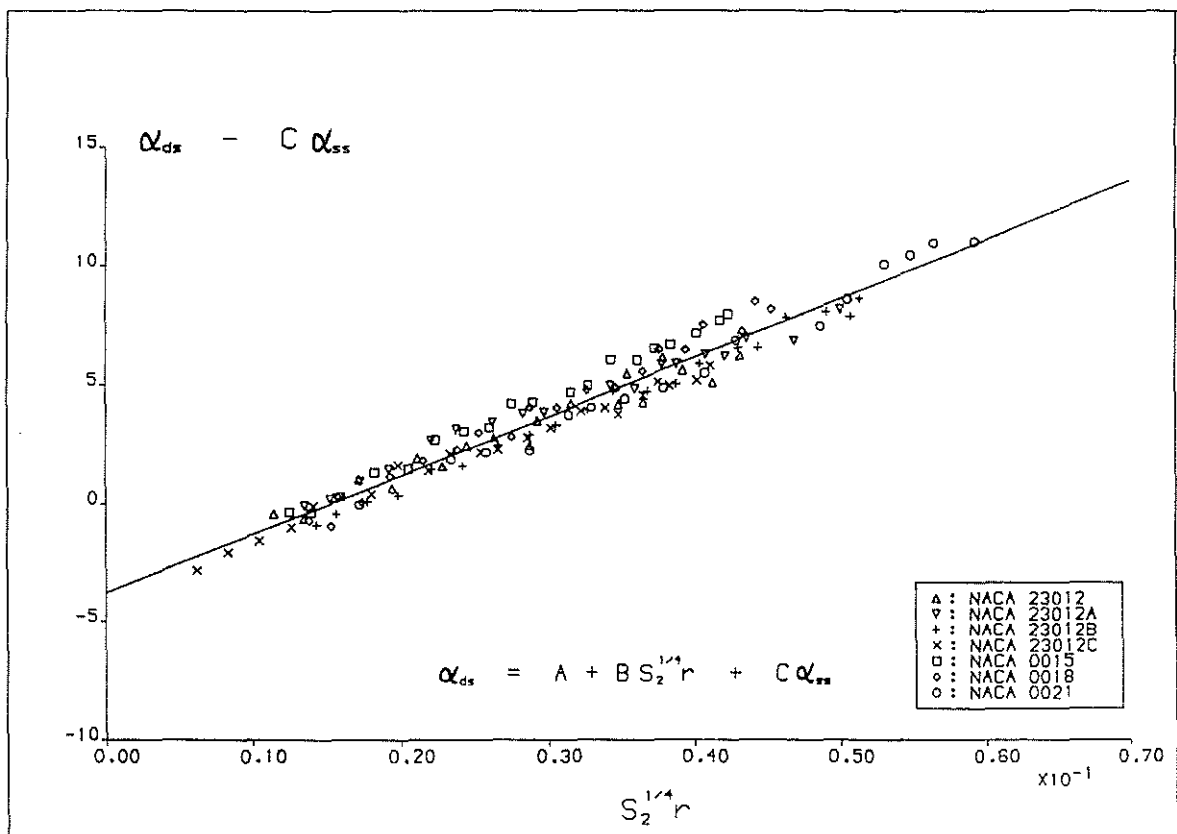
Figure 12   Dynamic Stall Correlation based on Dynamic Data only
$$Re = 1.5 \times 10^6, M_\infty = 0.11$$

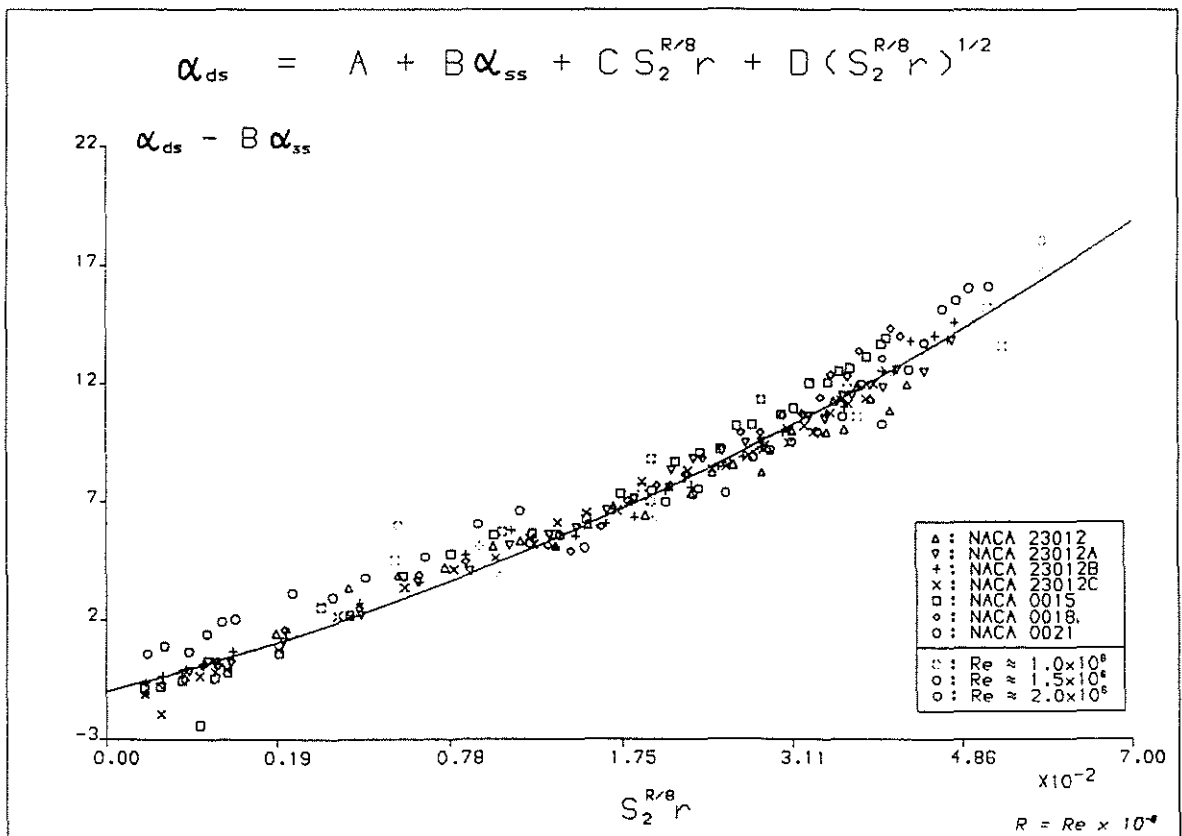$$\alpha_{ds} = A + B\alpha_{ss} + C S_2^{1/4} r + D(S_2^{1/4} r)^{1/2}$$
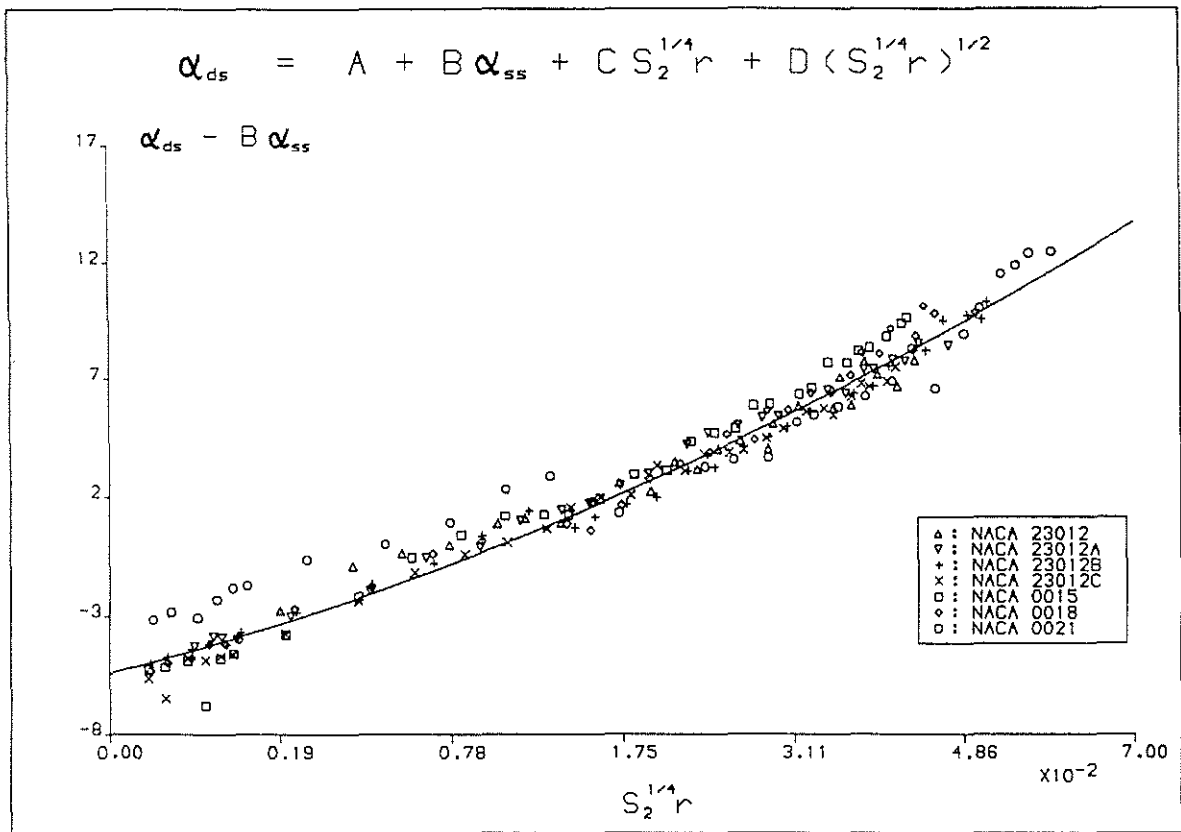
Figure 13   Dynamic Stall Correlation based on Quasi-Static and
Dynamic Data, Re = 1.5 x 10⁶, M∞ = 0.11

$$\alpha_{ds} = A + B\alpha_{ss} + C S_2^{R/8} r + D(S_2^{R/8} r)^{1/2}$$

Figure 14   Final Dynamic Stall Correlation
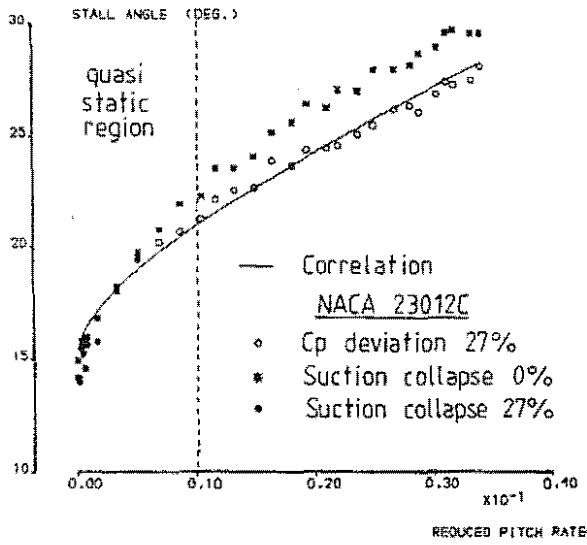
Figure 15   Comparison between Final Dynamic
Stall Correlation and Various
Chordwise Pressure Events
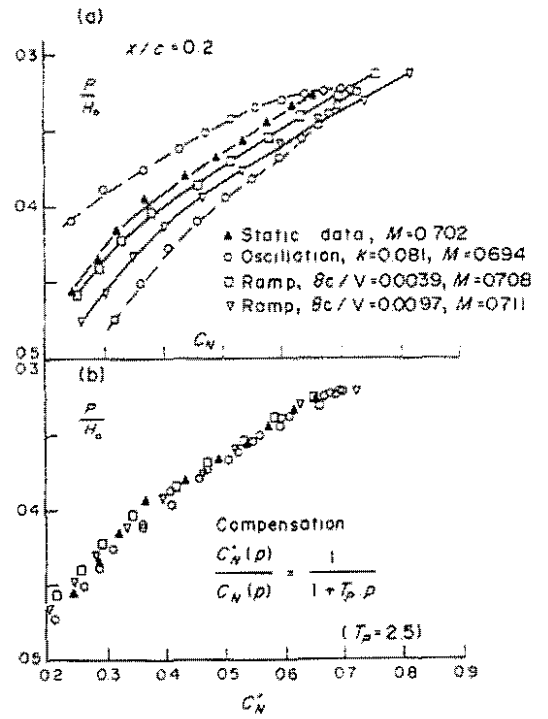
Figure 16   Compensation of Time Dependent
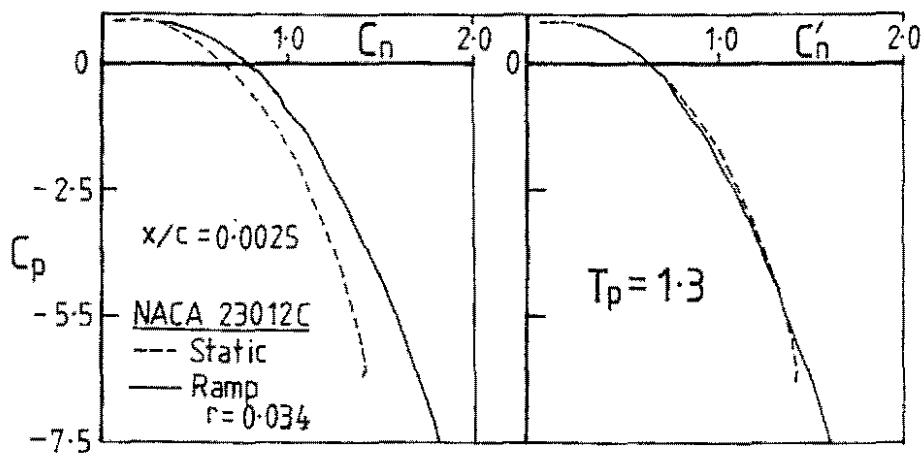Pressures (from Beddoes [24])

Figure 17   Tp Calculation for NACA 23012C
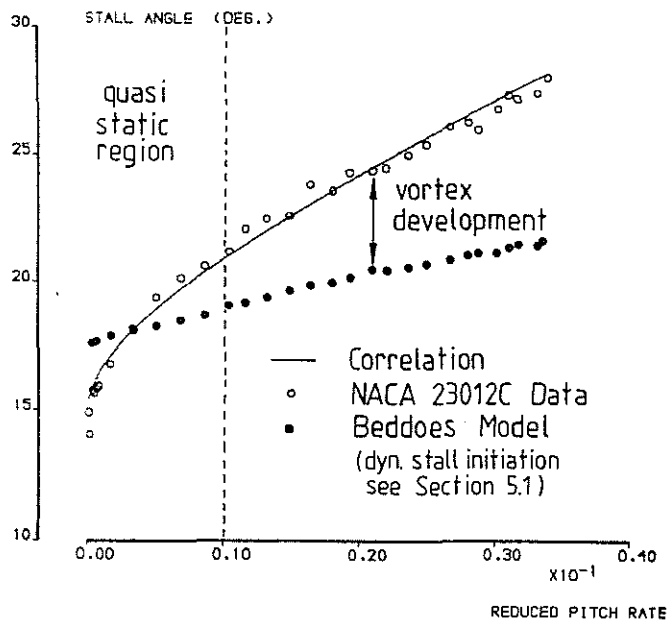$Re = 1.5 \times 10^6$, $M_\infty = 0.11$

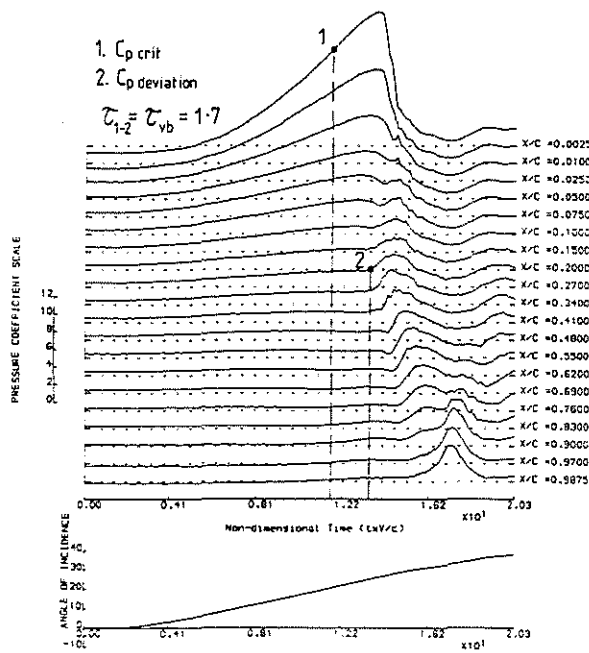**Figure 18   Comparison between Final Dynamic Stall Correlation and Beddoes Model**

Figure 19   Vortex Development Time Delay NACA 23012C, Ramp Test, r = 0.021

$$Re = 1.5 \times 10^6, M_\infty = 0.11$$

11-022